Conduction electrons in aperiodic versus periodic structures: An ESR study of quasicrystalline *i*-Y(Gd)-Cd and its approximant Y(Gd)Cd_6

M. Cabrera-Baez,[1,2] M. A. Avila,[3] and C. Rettori[1,3]
[1]*Instituto de Física "Gleb Wataghin," UNICAMP, Campinas, SP, 13083-859, Brazil*
[2]*Departamento de Física, Universidade Federal de Pernambuco, Recife, PE, 50670-901, Brazil*
[3]*CCNH, Universidade Federal do ABC (UFABC), Santo André, SP, 09210-580, Brazil*

(Received 18 December 2018; revised manuscript received 3 May 2019; published 31 July 2019)

A formal description of collective electronic states in condensed-matter systems lacking long-range periodicity remains a theoretical challenge. To experimentally explore the differences in electronic and magnetic behavior between metallic quasicrystals (QCs) and their conventional crystalline analogs [quasicrystal approximants (QCAs)], we have grown single crystals of $Y_{1-x}Gd_xCd_6$ (QCA) together with their QC counterparts *i*-$Y_{1-x}Gd_x$-Cd for $x = 0.006$, 0.01, 0.1, and 1.00, and we carried out comparative T-dependent electron spin resonance (ESR) measurements. On the high Gd concentration side, $x = 1.00$, we confirm that $GdCd_6$ adopts an antiferromagnetic ground state below $T_N \sim 22$ K, whereas *i*-Gd-Cd presents spin-glass-like behavior showing similar local and dynamical properties from the point of view of ESR. For the diluted samples, our ESR experimental results show similar local conduction electron polarization behavior at the Gd^{3+} site in all QC/QCA pairs investigated, supporting the validity of using QCAs as periodic representations of QCs in terms of short-range electronic interactions. However, there is a measurable difference in the Korringa relaxation rate (spin-flip relaxation process between the localized $Gd^{3+}4f$ electron and the delocalized s-type conduction electrons at the Fermi surface) between the QC/QCA pairs probably associated with the lack of periodicity. We expect that our comparative ESR study may provide support and motivation for the development of new theoretical approaches toward a *generalized band-structure* theory, contemplating condensed-matter systems beyond the scope of traditional periodicity.

DOI: 10.1103/PhysRevB.100.014207

I. INTRODUCTION

Solid-state physics offers the possibility of studying local and collective quantum phenomena at the atomic scale. Over the decades, various models have been developed and improved to offer reasonable explanations of these quantum phenomena under certain specific conditions [1,2]. Most of the modeling approaches in solid-state physics rely on the system periodicity, which leads to powerful descriptions such as the electronic band structures in compounds, based on Bloch's theorem. With the evolution of research and technology, previously unknown materials and structures are regularly envisaged or discovered, and the complexity of these systems tends to increase, leading to intriguing new quantum phenomena and the demand for new and better modeling of the involved physics. An outstanding class of such complex materials are those with quasicrystalline structures, typically found in certain metallic alloys that manifest features forbidden for conventional crystalline lattices, such as aperiodic long-range structural order and fivefold/tenfold rotational symmetries. Quasicrystals (QCs) were discovered in 1982 [3], and since then significant efforts have been made to understand how the lack of periodicity affects the thermodynamic, electronic, and magnetic properties, among others.

One striking issue found within this class is the disappearance of long-range magnetic order observed in certain QCs, whose crystalline counterparts—known as quasicrystal approximants (QCAs)—feature magnetically ordered ground states. The understanding of this phenomenon in QCs involving $3d$ transition metals (TMs), such as their aluminum-based alloys (Al-TM), is made difficult due to the poorly localized nature of their magnetic moments [4,5]. In fact, the very concept of a delocalized electron in an aperiodic lattice already constitutes a challenge, if its wave function is to vanish at the ionic lattice positions as usual. Systems containing $4f$ rare earths may be better described due to their highly localized magnetic moments, which can interact via the Ruderman-Kittel-Kasuya-Yosida (RKKY) mechanism, which nonetheless must be mediated by delocalized conduction electrons. Note that standard RKKY interactions depend on the distance between the local magnetic moments, and the modeling relies on the oscillation of the conduction electron polarization, which is associated with the Fermi wave vector [6]. The latter is formally undefined in quasicrystals, since the fundamental concepts of a Brillouin zone and a Fermi surface cannot be applied to them in the conventional way [7–9].

A powerful experimental technique that can be used to explore metallic systems in general from a microscopic point of view is electron spin resonance (ESR), which makes use of a natural or implanted magnetic local probe (the spin of an atom containing f- or d-type localized electrons) to extract information about its microscopic environment through the magnetic interactions between that probe and the system conduction electrons [10]. Very few studies have been conducted so far in this class of materials using the ESR technique,

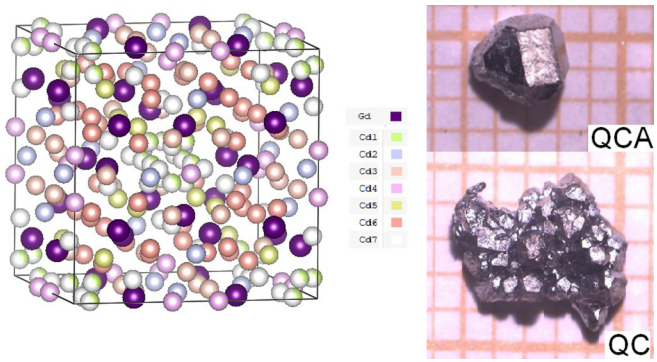

FIG. 1. Left: representation of the cubic unit cell of $GdCd_6$ ($a \approx 15.536$ Å). Right: photo of a typical cubic-shaped single crystal of $GdCd_6$ (QCA) and the quasicrystal *i*-Gd-Cd (QC) on millimeter paper.

one example being an investigation of the $Al_{63}Cu_{25}Fe_{12}$ QC [11]. An extremely broad resonance (4–5 T) was observed and attributed to conduction electrons and localized *d*-type electrons at almost the same resonance field, in which case it becomes very difficult to extract the relevant ESR parameters for proper interpretation of the interactions involved.

To investigate the subtle differences that may arise between QCs and QCAs in their electronic and magnetic properties, we have chosen as a stable and tractable system the recently discovered series of rare-earth-based binary intermetallic compounds *i*-*R*Cd (R = Y,Gd-Tm) [12].

The corresponding QCA of this family has a body-centered-cubic (bcc) crystal structure ($Im\bar{3}$) (see Fig. 1) and is composed of a so-called Tsai-type icosahedral cluster considered as the building blocks of the quasicrystals [13].

This proximity at the microscopic to mesoscopic level allows for comparative studies of the physical properties associated with the role of the periodicity or the lack thereof [14].

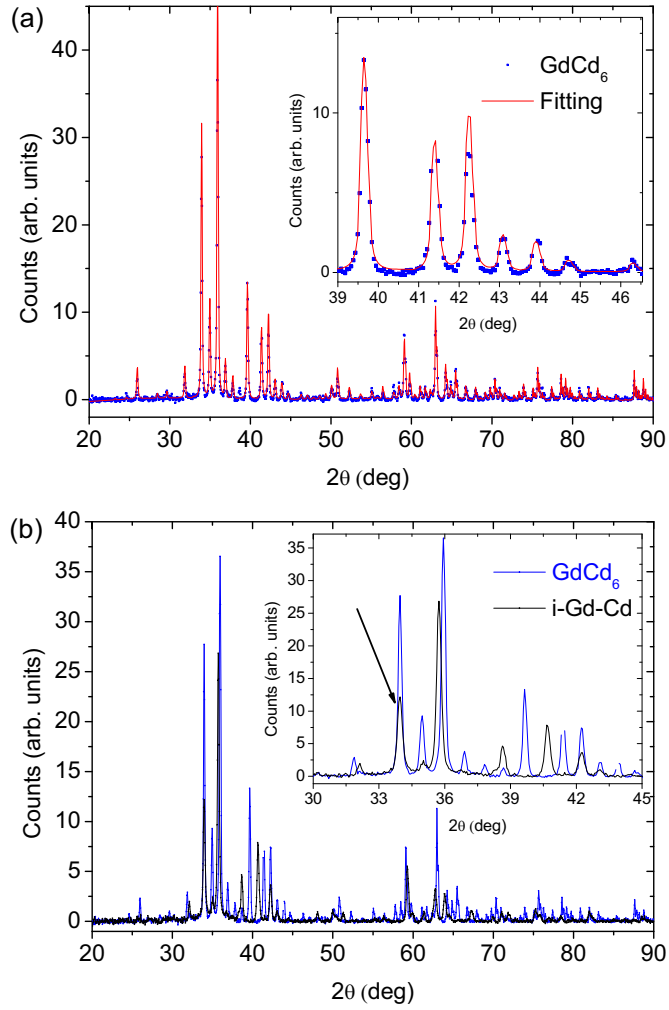

FIG. 2. (a) XRD pattern of powdered $GdCd_6$ crystals and inset showing the adjustment of the experimental data with the expected structure. (b) Comparative of the XRD pattern for $GdCd_6$ and *i*-Gd-Cd. The arrow in (b) indicates the fivefold axis indexed as (211111).

II. EXPERIMENTAL DETAILS

With the purpose of getting a deeper understanding of the electronic properties of QCs, batches of $Y_{1-x}Gd_xCd_6$ QCAs (used as a reference) and *i*-$Y_{1-x}Gd_xCd_6$ QCs with $x = 0$, 0.006, 0.01, 0.10, and 1.00 single and quasicrystals were grown by the standard self-flux method [15,16] using an excess of Cd following the reformulated phase diagram including the recently discovered QC phase *i*-*R*-Cd as described previously [12]. The constituent elements were 99.99% Y (Ames), 99.9% Gd, and 99.9999% Cd (Alfa-Aesar). For the magnetic susceptibility ($\chi = M/H$) measurements, we use a Quantum Design Superconducting Quantum Interference Device magnetometer MPMS3-SQUID platform at various applied magnetic fields ($H \leqslant 3$ T) and temperatures ($2.0 \leqslant T \leqslant 310$ K). The Gd concentration was estimated through dc magnetic susceptibility measurements using the Gd^{3+} effective magnetic moment [17] $\mu_{\text{eff}} = 7.94\mu_B$. The stoichiometry used for the calculation in the QCs was adopted from the wavelength dispersive spectroscopy (WDS) results reported in Ref. [12], $YCd_{7.48}$ for *i*-Y-Cd and $GdCd_{7.88}$ for *i*-Gd-Cd [18]. The estimated Gd concentration is in very good agreement with the nominal one for each sample.

For the ESR experiments, samples were crushed into fine powders of particle size greater than 100 μm, corresponding to an average grain size (d) larger than the skin depth (δ), $\lambda = d/\delta \gtrsim 10$. The X-Band ($\nu \approx 9.4$ GHz) ESR experiments were carried out in a conventional CW Bruker-ELEXSYS 500 ESR spectrometer using a TM_{4103} cylindrical cavity. The sample temperature was changed using a helium gas-flux coupled to an Oxford T-controller.

III. EXPERIMENTAL RESULTS

The phase of the QCA was confirmed using the usual method of x-ray diffraction (XRD) experiments and the patterns fitted to the structure observed previously [14]. However, in the absence of a conventional identification diffraction index for the QC, the obtained diffraction patterns were confronted with the pioneering work for these compounds [12,18].

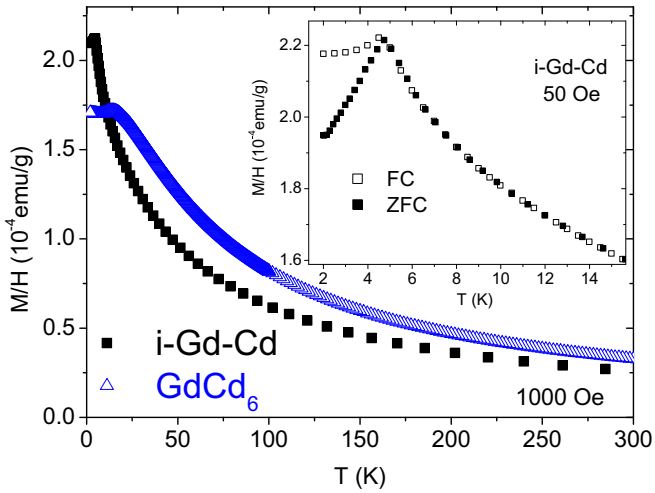

FIG. 3. Temperature dependence of the dc magnetic susceptibility for $GdCd_6$ (blue triangles) and *i*-Gd-Cd (black squares) under applied field $H = 1000$ Oe and 50 Oe (inset) for the quasicrystal.

Figure 2(a) displays the XRD diffraction pattern of $GdCd_6$ appropriate to the bcc cubic structure (inset, space group $Im\bar{3}$) with a lattice parameter of $a = 15.536$Å consistent with reported data [14]. Figure 2(b) shows a comparison between the diffraction peaks obtained for $GdCd_6$ and for *i*-Gd-Cd. The obtained peaks for the QC are in good agreement with reported XRD results [18]. The arrow in Fig. 2(b) indicates the fivefold axis indexed as (211111) in a previous report [12,18], which gives us confidence about the synthesis of our grown QCs. The associated structure in both systems is preserved as Gd is incorporated in the compound, in agreement with previous results [12,18].

To further support our XRD phase identification, dc magnetic susceptibility gives independent confirmation of the quality of our single and quasicrystals, revealing antiferromagnetic (AFM) correlations in QCAs and the absence of magnetic ordering in the QC as described in the main text.

Figure 3 presents the T-dependent dc-magnetic susceptibility response for $GdCd_6$ and *i*-Gd-Cd. As expected, a Curie-like behavior is seen in both at high-T, but there are strong differences at low-T. In agreement with the literature [12], AFM ordering is found for the QCA and spin-glass-like behavior for the QC (inset of Fig. 3).

To explore, microscopically, the involved magnetic couplings in our comparative study of QCs and QCAs, we have performed ESR experiments in $Y_{1-x}Gd_xCd_6$ and *i*-$Y_{1-x}Gd_x$-Cd single and quasicrystals with $x = 0$, 0.006, 0.01, 0.10, and 1.00, at several temperatures.

Starting with the concentrated system at room-T and $P_{\mu w} = 2$ mW, the observed ESR spectra of Gd^{3+} in $GdCd_6$ and *i*-Gd-Cd have Dysonian line shapes [Fig. 4(a)], typical of metallic systems. These were fitted [19] (red solid line), and the two relevant parameters of the ESR spectra, namely the resonance field $H_{\rm res}$ (related to the g-shift Δg) and the linewidth (ΔH), were extracted. The same experiments and fittings were then carried out as a function of temperature down to 4 K.

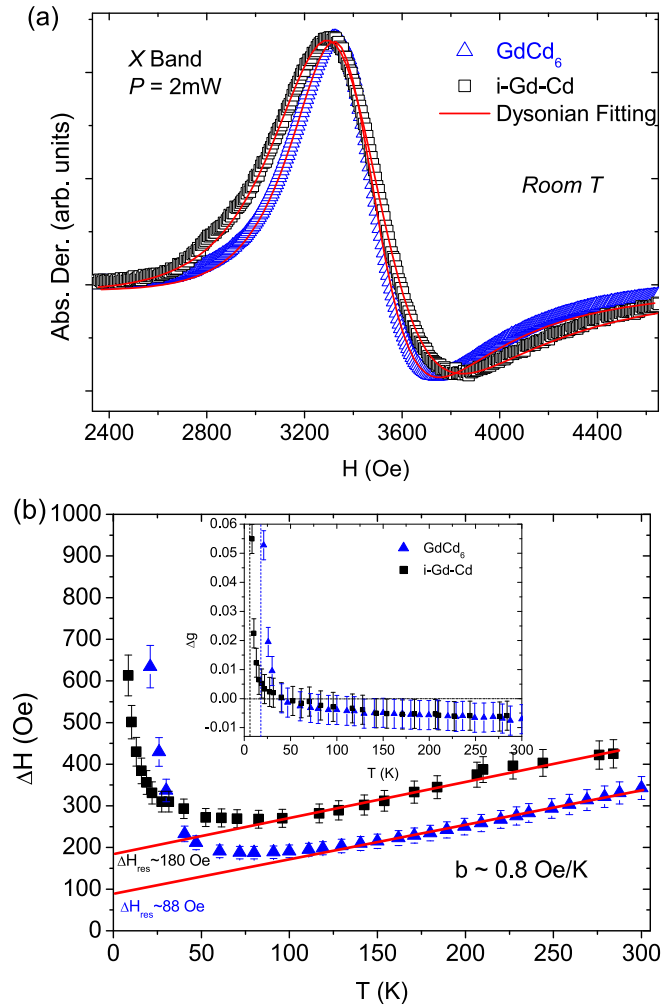

FIG. 4. (a) Resonance of Gd^{3+} spin in $GdCd_6$ and *i*-Gd-Cd at room-T. (b) Temperature dependence of the extracted ESR linewidth ΔH and g-shift Δg (inset).

The T-dependence of the linewidth (ΔH versus T) is given in Fig. 4(b). In the paramagnetic regime, the linewidth follows a linear T-dependence, $\Delta H = \Delta H_{\rm res} + bT$, where $\Delta H_{\rm res}$ is the residual linewidth and $b = d(\Delta H)/dT$ is the Korringa-like relaxation rate. Note that in the Gd concentrated systems, the b parameter is the same, $b = 0.8$ Oe/K, i.e., for both periodic $GdCd_6$ and aperiodic *i*-Gd-Cd. Moreover, at all T the absolute linewidth, including the residual linewidth $\Delta H_{\rm res}$, is broader for the QC than for the QCA, presumably associated with local (structural and/or magnetic) inhomogeneities of aperiodic systems.

For both systems, Δg shows similar T-independent negative values at high-T (paramagnetic regime) $\Delta g = -0.008(3)$, however a strong deviation toward positive g-shift takes place at low-T [inset of Fig. 4(b)], signaling the presence of an extra local T-dependent short-range FM field. The strength of this extra FM field, presumably due to an RKKY-like interaction, is different in both systems where, below $T \lesssim 50$ K, the T-dependence of Δg in the QCA is stronger (blue triangles) than that of the QC (black squares), consistent with the magnetic susceptibility of Fig. 3.

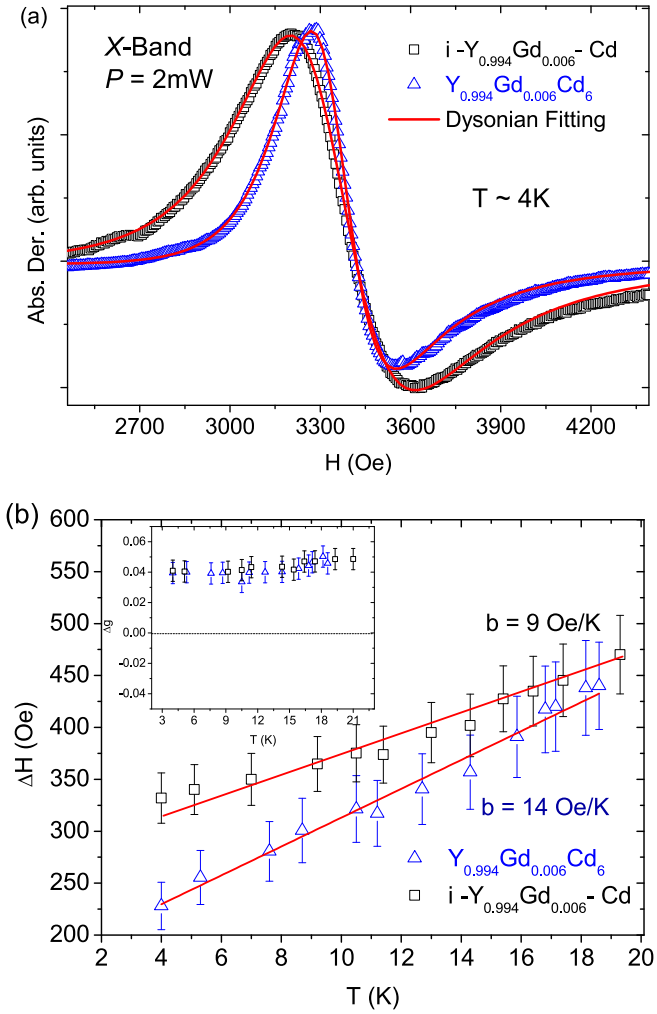

FIG. 5. (a) Resonance of Gd^{3+} spin in $Y_{0.994}Gd_{0.006}Cd_6$ and i-$Y_{0.994}Gd_{0.006}$-Cd at $T = 4$ K. (b) Temperature dependence of the extracted ESR linewidth ΔH and g-shift Δg (inset).

As the b parameter may be affected by the concentration of the magnetic ion (bottleneck effect [20]) due to the Overhauser mechanism [21], proper correlation of the measured Korringa-like rate with the intrinsic Korringa relaxation rate [22] of these systems demands investigation of diluted Gd^{3+} in i-Y-Cd quasicrystals and its approximant YCd_6.

The ESR spectra of Gd^{3+} in $Y_{0.994}Gd_{0.006}Cd_6$ and i-$Y_{0.994}Gd_{0.006}$-Cd at $T = 4$ K are displayed in Fig. 5, where a clear difference in the T-evolution of the linewidth is observed at a glance: ΔH becomes larger at low-T for the QC than for the QCA, evidencing fundamental differences in the intrinsic Korringa relaxation rate [see Fig. 5(b)]. Notice also the large difference in thermal broadening of the linewidth between these diluted limits and the concentrated ones (Fig. 4). For both systems, Δg versus T shows almost the same value (see the upper inset of Fig. 5).

Similar behavior was also observed for the QC/QCA pair i-$Y_{0.99}Gd_{0.01}$-Cd and $Y_{0.99}Gd_{0.01}Cd_6$, respectively, for which the full set of extracted parameters ΔH versus T and Δg versus T (inset) at several temperatures between 4 and 19 K are shown in Fig. 6. Contrary to the concentrated systems

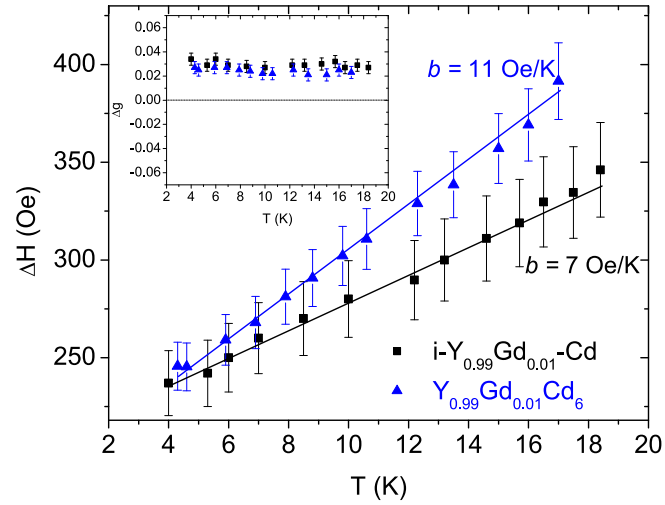

FIG. 6. Extracted linewidth ΔH and g-shift Δg (inset) as a function of temperature for 1% diluted Gd^{3+} in i-Y-Cd quasicrystal and approximant YCd_6.

behavior, $\Delta g = 0.027(3)$ is positive and T-independent for both systems in this temperature range. Nonetheless, a measurable difference occurs in the Korringa-like relaxation rate, $b = 11.1(5)$ Oe/K for the QCA and $b = 7.0(5)$ Oe/K for the QC. Hence, these results also indicate a subtle, yet fundamental, difference in the spin relaxation mechanism between the ordered QCA and aperiodic QC.

Finally, the experiments were repeated for a slightly more concentrated QC/QCA pair, i-$Y_{0.9}Gd_{0.1}$-Cd and $Y_{0.9}Gd_{0.1}Cd_6$. The ESR parameters Δg and b remain about the same for both systems, similar to the concentrated samples although at different concentration values. Table I summarizes the ESR parameters for all the studied QC/QCA pairs.

IV. ANALYSIS AND DISCUSSION

In preparation for the analysis of the ESR data of Table I, let us first discuss the physical meaning of the Δg and b parameters. Within a molecular field approximation, the g-shift is given by the shift of the Gd^{3+} resonance field due to a local magnetic field, produced by the exchange interaction with the conduction electrons polarization, $J_{fce}(k_F^{\text{out}}, k_F^{\text{in}}) = J_{fce}(0)$, in the absence of conduction electron momentum transfer at the Fermi surface, i.e., $k_F^{\text{out}} = k_F^{\text{in}}$. The thermal broadening of the linewidth, b (Korringa-like rate), however, is associated with the conduction electrons and Gd^{3+} spin-flip scattering via an exchange interaction at the Fermi surface $J_{fce}(\vec{k}_F^{\text{out}}, \vec{k}_F^{\text{in}}) =$

TABLE I. Summary of all ESR parameters obtained for $Y_{1-x}Gd_xCd_6$ (QCA) and i-$Y_{1-x}Gd_x$-Cd (QC).

x	Δg (QCA)	Δg (QC)	b (QCA)	b (QC)
0.006	0.040(3)	0.044(3)	14.0(6)	9.0(7)
0.01	0.027(3)	0.027(3)	11.1(5)	7.0(5)
0.10	−0.001(3)	0.003(3)	5.9(5)	5.9(5)
1.00	−0.008(3)	−0.008(3)	0.8(5)	0.8(5)

$J_{fce}(|\vec{k}_F^{\rm out} - \vec{k}_F^{\rm in}|) = J_{fce}\{q = k_F[2(1-\cos\theta)]^{1/2}\}$, i.e., in the presence of conduction electron momentum transfer, $0 \lesssim q \lesssim 2k_F$, at the Fermi surface [23].

Table I indicates that the g-shift of both systems, QC and QCA, behaves similarly, meaning that the conduction electron polarization is reasonably equivalent at the local Gd^{3+} sites, regardless of the Gd concentration. However, there is an evident sign change of Δg as the Gd concentration increases, being positive at low concentrations and negative at high concentrations with a crossover at $x \approx 0.10$. This implies that the analysis of our ESR data must take into account the band structure of these compounds, involving contributions of different types of conduction electrons at the Fermi level. In fact, DFT calculations in the YCd_6 QCA have revealed the existence of s-, p-, and d-type conduction electrons at the Fermi level and no strong electron-electron correlations [24].

In contrast with the g-shift behavior, for the b parameters Table I shows that there is a fundamental difference at low Gd concentration between the QC and QCA compounds. These results demonstrate that the ESR technique has proven capable of detecting a subtle difference between these compounds with respect to the Gd^{3+}-conduction electron spin-flip scattering processes. So, in the analysis of our ESR data it will be necessary to consider the q-dependence of the exchange interaction [23] and also the possibility of the presence of a *bottleneck* phenomenon [20] (see the Appendix) due to the Overhauser mechanism [21].

At first approximation, a multiband analysis of the ESR data for metallic compounds such as the QCA $Y_{1-x}Gd_xCd_6$ leads to Δg and b given by

$$\begin{aligned}\Delta g &= \Delta g_{fs} + \Delta g_{fp} + \Delta g_{fd} \\ &= J_{fs}(0)\eta_{F_s} - J_{fp}(0)\eta_{F_p} + J_{fd}(0)\eta_{F_d} \end{aligned} \quad (1)$$

and

$$\begin{aligned} b &= \frac{\pi k_B}{g\mu_B}\left[F_s\Delta g_{fs}^2 + F_p\Delta g_{fp}^2 + F_d\Delta g_{fd}^2\right] \\ &= \frac{\pi k_B}{g\mu_B}\left[F_s\langle J_{fs}^2(q)\rangle_F\eta_{F_s}^2 + F_pJ_{fp}^2(0)\eta_{F_p}^2 + F_dJ_{fd}^2(0)\eta_{F_d}^2\right], \end{aligned} \quad (2)$$

where k_B is the Boltzmann constant, μ_B is the Bohr magneton, and g is the Gd^{3+} g-value; $J_{fi}(0)$ $(i = s, p, d)$ are the effective $q = 0$ components of the exchange interaction between the Gd^{3+} $4f$ localized magnetic moment and the s-, p-, and d-type of ce; η_{F_i} $(i = s, p, d)$ is the partial *bare* DOS (states/f.u., spin, and eV) at the Fermi level of the s-, p-, and d-type ce; $\langle J_{fs}^2(q)\rangle_F$ is the average over the Fermi surface of the square of the q-dependent effective exchange parameter in the presence of ce momentum transfer, $q = |\vec{k}_{\rm out} - \vec{k}_{\rm in}|$, i.e., $\langle J_{fs}(q)\rangle_F \neq J_{fs}(0)$ [23]. $F_s = 1$, $F_p = 1/3$, and $F_d = 1/5$ are factors associated with the orbital degeneracy of the unsplit (no crystal-field effects) bands at the Fermi level, respectively. The q-dependence of the exchange interaction with the p- and d-type ce will be ignored due to their higher localization as compared with the strongly itinerant s-type conduction electrons, making unlikely the spin-flip scattering at the Fermi surface by those types of conduction electrons, i.e., $\langle J_{fp,d}(q)\rangle_F = J_{fp,d}(0)$ (see below). In Eqs. (1) and (2), we have considered that the contribution to Δg due to the exchange interaction with s- and d-type ce is positive (atomiclike) and that with p-type ce is negative (covalentlike) [23].

Due to the strong spin-orbit coupling of p- and d-type ce compared to that of the s-type ce, we make the usual assumption that only the s-type ce are capable of experiencing the *bottleneck* effect. Hence, we can consider that the contribution of the s-type ce to the ESR parameters, Δg-shift, and b is negligible for samples with high Gd^{3+} concentration. Moreover, in general, the q-dependence of the exchange parameters $J(q)_{f,i}$ $(i = s, p, d)$ must be accounted for. However, in cases in which the relaxation rate b is of the order of what is expected from the g-shift $[b = (\pi k_B/g\mu_B)(\Delta g)^2]$, one can neglect the q-dependence of the exchange parameters, i.e., $J(q)_{fp} = J(0)_{fp}$ and $J(q)_{fd} = J(0)_{fd}$. In our case, for $x = 1.00$ ($GdCd_6$ and i-Gd-Cd) we found 0.8(5) Oe/K $\approx 2.34 \times 10^4$ (Oe/K) $\times [-0.008(3)]^2 \approx 1.5(6)$ Oe/K, which is similar, within the accuracy of our measurements. Thus, with these assumptions, for $x = 1.0$ in the extreme *bottleneck* regime Eqs. (1) and (2) reduce to

$$\Delta g = -0.008(3) = -J_{fp}(0)\eta_{F_p} + J_{fd}(0)\eta_{F_d} \quad (3)$$

and

$$b = 0.8(5)\ \text{Oe/K} = \frac{\pi k_B}{g\mu_B}\left[F_pJ_{fp}^2(0)\eta_{F_p}^2 + F_dJ_{fd}^2(0)\eta_{F_d}^2\right]. \quad (4)$$

Using the total density of states of s-, p-, and d-type conduction electrons at the Fermi level, $\eta_{fce} = \eta_{F_s} + \eta_{F_p} + \eta_{F_d}$, given by the band-structure calculations for YCd_6 (QCA) [24] and within a free-electron model, we estimate a Sommerfeld coefficient of $\gamma = 2.0(1)$ mJ/mol K^2. This is somewhat smaller than the reported experimental value [14,18] $\gamma = 9(4)$ mJ/mol K^2 for YCd_6 QCA and similar to that reported for the i-Y-Cd QC $\gamma = 4(2)$ mJ/mol K^2. Hence, taking into consideration the experimental accuracies and model approximations, as far as the density of states at the Fermi level is concerned, there is not much difference between the QC/QCA pair i-Y-Cd and YCd_6. However, it is important to recall that a density of states at the Fermi level, and Fermi surfaces in general, have only been formally defined for periodic systems, so the experimentally obtained Sommerfeld coefficient $\gamma^* = (C_p/T)|_{T^2\to 0}$ may not be directly associated with the density of states, η_F, in the traditional manner. From these considerations, we use Eqs. (3) and (4) for $x = 1.0$ ($GdCd_6$ and i-Gd-Cd) assuming a similar type of conduction electron participation. Then, for $\eta_{F_d} = 0.153$ states/f.u., spin and eV, and $\eta_{F_p} = 0.176$ states/f.u., spin and eV [24], we estimate $J_{fp}(0) = 57(6)$ meV and $J_{fd}(0) = 13(5)$ meV for QCA and QC systems, respectively.

On the other hand, in the *unbottleneck* regime (lowest Gd concentration, $x \approx 0.006$ in Table I) for both systems, Eqs. (1) and (2) reduce to

$$\Delta g = 0.040(2) = J_{fs}(0)\eta_{F_s} - 0.008(3), \quad (5)$$

$$b = 14.0(6)\ \text{Oe/K} = \frac{\pi k_B}{g\mu_B}\left[F_s\langle J_{fs}^2(q)\rangle_F\eta_{F_s}^2\right] + 0.8(5) \quad (6)$$

for the QCA and

$$\Delta g = 0.044(3) = J_{fs}(0)\eta_{F_s} - 0.008(3), \quad (7)$$

$$b = 9.0(7)\ \text{Oe/K} = \frac{\pi k_B}{g\mu_B}\left[F_s\langle J_{fs}^2(q)\rangle_F \eta_{F_s}^2\right] + 0.8(5) \quad (8)$$

for the QC.

Using $\eta_{F_s} = 0.084(1)$ states/f.u., spin and eV [$\eta_{Fs} = \eta_{fce} - (\eta_{F_p} + \eta_{F_d})$] [24], we obtain $J_{fs}(0) = 571(17)$ meV and $\langle J_{fs}^2(q)\rangle_F^{1/2} = 283(19)$ meV for the QCA and $J_{fs}(0) = 620(16)$ meV and $\langle J_{fs}^2(q)\rangle_F^{1/2} = 223(17)$ meV for the QC.

Still, the essence of our experimental data is a similar g-shift for all QC/QCA pairs indicating closely related local conduction electron polarization at the Gd^{3+} site, which is a remarkable microscopic result leading to equally comparable values for the exchange parameter, $J_{fce}(0)$. In contrast, notably different Korringa parameters, b, were found when QC and QCA are compared in the low Gd concentration limit, i.e., in the *unbottleneck* regime where s-types of conduction electrons also participate in the relaxation process. Notice that in Table I the bottleneck regimes are opened at about the same Gd concentrations in both systems, $0.01 < x < 0.10$, indicating that the s-type of conduction electron–lattice relaxation is not too different. Therefore, their different b values may be exclusively attributed to the exchange interaction Gd-conduction electrons averaged over the Fermi surface $\langle J_{fs}^2(q)\rangle_F^{1/2}$ suggesting that the lack of periodicity should lead to a smaller renormalized-like QC Fermi surface. The Korringa relaxation rate is associated with the dynamics of conduction electron momentum transfer via Gd^{3+}-conduction electron spin-flip exchange scattering at the Fermi surface.

One may then expect to see changes in this parameter in QC systems due to the ill-defined concept of a Fermi surface in such cases. Our analysis at low Gd concentration shows that, assuming the contribution of s-type conduction electrons to the DOS remains the same, the Korringa rate for the QC is suppressed when compared to its QCA counterpart, implying a smaller $\langle J_{fs}^2(q)\rangle_F^{1/2}$ for the QC.

We propose that the observed differences in the Korringa-like parameter evidence the need for a new and broader definition of Fermi surface that we might tentatively refer to as the *generalized Fermi surface*, appropriate to describe electronic and magnetic behavior in complex structural arrangements of atoms, including QC systems such as our i-Y-Cd. In such a case, the traditionally defined Fermi surface would remain as a special case valid for long-range periodic structures. It is likely that first-order perturbation theory may offer a useful initial steps toward this goal, at least in the case of QC.

V. CONCLUSIONS

Our ESR experimental results show similar local conduction electron polarization behavior at the Gd^{3+} site in all QC/QCA pairs investigated, supporting the validity of using QCA as periodic representations of QC in terms of short-range electronic interactions. However, a fundamentally important difference in the Gd^{3+} spin relaxation process involving conduction electrons was resolved between the family of binary icosahedral quasicrystals i-R-Cd and their quasicrystal approximants RCd_6 (R = Gd,Y). This difference in the Korringa relaxation rate (difference in the Gd^{3+} spin-flip relaxation process between the localized f-electron and the delocalized s-type of conduction electrons at the Fermi surface) between QC/QCA pairs is associated with the lack of periodicity.

Given the delocalized nature of the s-type conduction electrons, we attribute the observed difference to the fact that such delocalized electrons are capable of feeling the lack of mid- to long-range periodicity in the QC, to which they adapt in the form of altered electronic quantum states that are as yet undescribed, to the best of our knowledge. An outstanding consequence should be the emergence of alternate magnetic ordering in aperiodic systems via new, but similar, forms of RKKY-type interaction, which, in the case of our i-Gd-Cd QC, leads to a spin-glass-like ground state rather than the AFM of its QCA, $GdCd_6$.

Therefore, it is expected that in the years to come, new theoretical approaches, contemplating condensed-matter systems beyond the scope of traditional periodicity, will be developed in order to describe the conduction electrons in a *generalized band-structure* theory that establishes more general definitions for Fermi levels, Fermi surfaces, densities of states at the Fermi level, etc., that will help in understanding and properly describing electron quantum states and dynamic processes in QC and other aperiodic systems.

Consequently, our results suggest that the Bloch wavefunction approach may be applied to i-(Y)Gd-Cd QC as long as the involved conduction electrons are more localized as p- and d-type. For more itinerant conduction electrons such as the s-type conduction electron, a more general approach than the Bloch theorem should be envisaged.

ACKNOWLEDGMENTS

This work was supported by Brazilian agencies FAPESP (Grants No. 2016/15780-0 and No. 2011/19924-2), CNPq, and CAPES.

APPENDIX

Exchange bottleneck phenomenon

Figure 7 presents an illustrative diagram very useful to understand the exchange bottleneck phenomenon presented

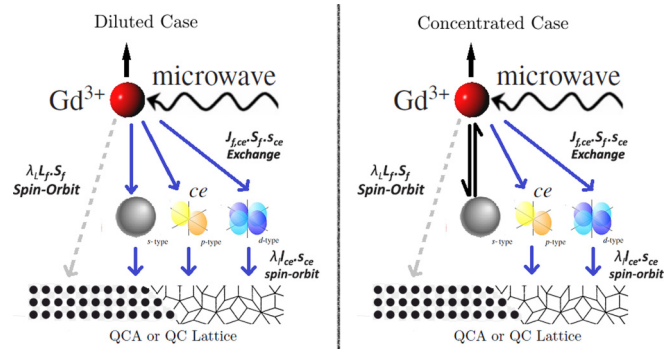

FIG. 7. Illustration for the transmission to the lattice of the microwave energy absorbed at resonance by the Gd^{3+} ions, assisted by the exchange interaction, $J_{fi}(\vec{S}_f \cdot \vec{s}_i)$ ($i = s, p, d$), between the Gd^{3+} ions and the s (*bottleneck*), p (*unbottleneck*), and d (*unbottleneck*) *ce*. Solid blue and black arrows indicate the easier and more difficult paths, respectively.

in the explored systems (QC and QCA). This figure indicates the easy and preferable paths (solid blue arrows) for the net flow of microwave energy (black curved arrow) absorbed at resonance by the Gd^{3+} ions to reach the QC or QCA lattice thermal bath. For the diluted case, there are three different paths going from Gd^{3+} ions to the lattice through conduction electrons via exchange interaction $[J_{fi}(\vec{S}_f \cdot \vec{s}_i)$ $(i = s, p, d)]$ between the Gd^{3+} ions and the s, p, and d *ce* and finally relaxing via spin-orbit coupling. However, this situation is different for the concentrated case, where Gd^{3+} ions and s-type conduction electrons are coupled and the flow of energy is in the *bottleneck* state for the s-type conduction electron (Overhauser mechanism). Since p- and d-type conduction electrons are incapable of experiencing the exchange bottleneck effect, due to their strong spin-orbit coupling, the only conduction electrons capable of undergoing the bottleneck [20] effect are the s-type conduction electrons.

[1] J. M. D. Coey, *Magnetism and Magnetic Materials* (Cambridge University Press, Cambridge, UK, 2009).

[2] K. H. J. Buschow, J. Less-Common Met. **43**, 55 (1975).

[3] D. Shechtman, I. Blech, D. Gratias, and J. W. Cahn, Phys. Rev. Lett. **53**, 1951 (1984).

[4] J. J. Hauser, H. S. Chen, and J. V. Waszczak, Phys. Rev. B **33**, 3577(R) (1986).

[5] W. W. Warren, H. S. Chen, and G. P. Espinosa, Phys. Rev. B **34**, 4902 (1986).

[6] M. Cabrera-Baez, A. Naranjo-Uribe, J. M. Osorio-Guillén, C. Rettori, and M. A. Avila, Phys. Rev. B **92**, 214414 (2015).

[7] S. Thiem and J. T. Chalker, Phys. Rev. B **92**, 224409 (2015).

[8] F. L. A. Machado, W. G. Clark, D. P. Yang, W. A. Hines, L. J. Azevedo, B. C. Giessen, and M. X. Quan, Solid State Commun. **61**, 691 (1987).

[9] F. L. A. Machado, W. G. Clark, L. J. Azevedo, D. P. Yang, W. A. Hines, J. I. Budnick, and M. X. Quan, Solid State Commun. **61**, 145 (1987).

[10] A. Abragam and B. Bleaney, *Electron Paramagnetic Resonance (EPR) of Transition Ions* (Clarendon, Oxford, 1970); S. E. Barnes, Adv. Phys. **30**, 801 (1981); R. H. Taylor, *ibid.* **24**, 681 (1975); T. Plefka, Phys. Status Solidi B **55**, 129 (1973).

[11] J. Dolinšek, D. Arčon, A. Zorko, M. Klanjšek, C. Saylor, L. C. Brunel, P. Brunet, and J. M. Dubois, Phys. Rev. B **65**, 064205 (2002).

[12] A. I. Goldman, T. Kong, A. Kreyssig, A. Jesche, M. Ramazanoglu, K. W. Dennis, S. L. Bud'ko, and P. C. Canfield, Nat. Mater. **12**, 714 (2013).

[13] A. P. Tsai, J. Q. Guo, E. Abe, H. Takakura, and T. J. Sato, Nature (London) **408**, 537 (2000).

[14] A. Mori *et al.*, J. Phys. Soc. Jpn. **81**, 024720 (2012).

[15] P. C. Canfield and Z. Fisk, Philos. Mag. **65**, 1117 (1992).

[16] R. A. Ribeiro and M. A. Avila, Philos. Mag. **92**, 2492 (2012).

[17] J. M. D. Coey, *Magnetism and Magnetic Materials* (Cambridge University Press, Cambridge, UK, 2009).

[18] T. Kong, S. L. Bud'ko, A. Jesche, J. McArthur, A. Kreyssig, A. I. Goldman, and P. C. Canfield, Phys. Rev. B **90**, 014424 (2014).

[19] F. J. Dyson, Phys. Rev. **98**, 349 (1955).

[20] C. Rettori, D. Davidov, G. Ng, and E. P. Chock, Phys. Rev. B **12**, 1298 (1975).

[21] A. W. Overhauser, Phys. Rev. **89**, 689 (1953).

[22] J. Korringa, Physica **16**, 601 (1950); H. Hasegawa, Prog. Theor. Phys. **21**, 483 (1959).

[23] D. Davidov, K. Maki, R. Orbach, C. Rettori, and E. P. Chock, Solid State Commun. **12**, 621 (1973); D. Davidov, C. Rettori, R. Orbach, A. Dixon, and E. P. Chock, Phys. Rev. B **11**, 3546 (1975).

[24] Y. Ishii and T. Fujiwara, J. Alloys Compd. **342**, 343 (2002).